Tele-petrography in the quantitative evaluation of petrophysical characteristics of reservoir rocks with the terra package: The case of sandstones

ASSALE Fori Yao Paul[1], DANUMAH Jean Homian[2], KOUAO Assiè François Aristide[1], MONDE Sylvain[1], and KPLOHI Yaba Hervé[3]

[1]Département de Géosciences Marines, UFR des Sciences de la Terre et des Ressources Minières, Université Félix Houphouet-Boigny, Abidjan, Côte d'Ivoire

[2]Centre Universitaire de Recherche et d'Application en Télédétection (CURAT), UFR des Sciences de la Terre et des Ressources Minières, Université Félix Houphouet-Boigny, Abidjan, Côte d'Ivoire

[3]PETROCI, Centre d'Analyses et de Recherche (CAR), Abidjan, Côte d'Ivoire

ABSTRACT: In the present work, the cement and/or matrix, pores, and grains present in sandstones were quantified by tele-petrography. The selected sandstones come from the superficial formations of Ivorian onshore basin and the deep formations of offshore basin. A total of six sandstones, three from each part of Ivorian basin, were analyzed. The tele-petrographic analysis consisted of processing the images of these sandstones taken under the natural light from petrographic microscope to the R software using the «**terra**» package. The results show that the quantification of sandstone components depends on the magnification of the microscope image, the grain size, and the sorting. At low and medium magnifications, a small number of images per rock is sufficient to evaluate the proportions of the components. At high magnifications, however, a large number of images are required as they tend to overestimate the proportions of grains at the expense of other components (porosity, cement, matrix) if the grains have a poorly sorted. The presence of phenocrysts accentuates these variations. However, if the sandstones have a well sorting, the proportions of components hardly vary from one image to another, whatever the magnification. The density curves and histograms reveal that the number of components on these curves depends on the proportions; the higher the proportion of a component the better it is represented. Low proportions remain invisible on the density curves. Remote sensing is therefore promising for the evaluation of the petrophysical properties of reservoir rocks.

KEYWORDS: Tele-petrography, R, Terra, Sandstone, Porosity, reservoir rocks.

1 INTRODUCTION

The "terra" package, which was developed by Hijmans [1], provides methods for manipulating geographic (spatial) data in "raster" and "vector" forms. It is a package open access of the R language that implements two types of data: **SpatRaster** and SpatVector. A SpatRaster object represents raster data, in one or more layers (variables) that can store several fundamental parameters that describe it. It is based on the GDAL library that allows reading and processing a very large number of geographical image formats, preferably.**tif** (Tagged Image File Format).

The present work consisted of manipulating the images from natural petrographic microscope lights as a SpatRaster object without a geographical reference system which we called "tele-petrography".

Tele-petrography is a concept that we are developing at the Geology, Mineral, and Energy Resources Laboratory of the University of Félix Houphouët Boigny (Côte d'Ivoire). It consists of processing images from natural microscope light or an ordinary camera using the terra package to quantify the different components of a rock.

It is therefore the set of remote sensing techniques used to quantify the physical properties of rocks from the radiation they emit or reflect. In the case of the study of sedimentary rock with a petrographic microscope, it is an indirect method that allows the different components present on the thin slide to be clearly distinguished. These components are:

- The cement which binds the grains together;
- The matrix, the fine fraction between the grains;
- The pores which are the spaces between the grains
- The grains, which are made up of minerals

Given the usefulness of pores in the oil industry, this new technique comes at the right time in its quantitative evaluation. For the first publication of this technique, we used sandstones from the Ivorian sedimentary basin. The main objective of this study is to understand the distribution of the different components present in sandstones by this indirect technique. The specific objectives are:

- To design petrographic thin sections of these rocks;
- To carry out natural light petrographic microscopy on each thin slide;
- Process the images with the terra package.

2 METHODOLOGY

The main material submitted to our study is composed of six (6) sandstone samples (sandstone1, sandstone2, sandstone3, sandstone4, sandstone5, and sandstone6). The first three sandstones were obtained from outcrops of ferruginous sandstone from the Ivorian onshore basin and the other three from reservoir rock cores from the Ivorian offshore basin. The methodology used for the analysis of these samples is petrographic thin-slice design, petrographic description, natural light image capture, processing, and analysis of the resulting data.

The thin-slice technique starts with the impregnation of rocks under vacuum with a blue-colored resin to fill the pore spaces of the rocks. After impregnation, the rocks are reduced to a thickness of 30 µm and glued onto slides and flaps.

The resulting petrographic slides are observed under the natural light of the petrographic microscope at medium and high magnification depending on the size of the grains. The aim is to describe the rock and count the different components present in each rock (cement, matrix, pores, and grains). The description consists of determining the mineralogical composition, the nature of the cement, the type of porosity, the sorting according to Maurice [2] and Gary [3], the maturity [3], [4], and the type of sandstone [5]. For each rock observed, microscopic images are taken and recorded in the "**tif**" format.

The different images obtained are imported using the **terra** package ([1], [6], [7]). This package has functions to create a SpatRaster from images using the raster function of the package. The default settings create a global raster data structure with a coordinate reference system of longitude/latitude and cells (pixels). In the present work, no coordinate reference system is used.

The plot function of the package provides multi-spectral SpatRasters composed of cells (pixels). The resulting rasters contain categorical data (cement, matrix, grains, and pores) that are digitally coded. These codes are grouped by colour interval, and the more explicit spectra (layers) of the rock components are merged into a SpatRaster to better differentiate the components (Equation 1).

$$\mathbf{Layer} = \frac{\sum_1^n \text{layer (i)}}{n} \qquad \text{(Equation 1)}$$

Layer: merged layers, **layer (i)**: elementary layer, **n**: number of merged layers.

The analysis of the SpatRaster obtained after fusion consists in plotting histograms and density curves of the different rock components as a function of the colorations. Subsequently, the sum of the cells and the proportions of the components occupying the different cells are determined; this makes it possible to determine the percentages of cement, matrix, pores, and grains in each image (Equations 2 and 3). The total proportions are the sum of the proportions of each image taken per sample (Equation 4).

$$\mathbf{S} = \sum_1^n \text{cells} \qquad \text{(Equation 2)}$$

$$\mathbf{\%X_i} = \frac{\sum_1^n x}{S} \qquad \text{(Equation 3)}$$

$$\%X = \frac{\sum_1^n \%El\acute{e}ment}{n}$$ (Equation 4)

With :

S: sum of the cells,
%X$_i$: proportion of each component (cement, matrix, pores, grains) in image i,
%X: average of the proportions of each component over all the images taken per rock.

3 RESULTS

3.1 PETROGRAPHIC DESCRIPTION OF THE SANDSTONES

3.1.1 SANDSTONE OF THE IVORIAN ONSHORE BASIN

The petrographic description of the ferruginous sandstones reveals a mineralogy composed of xenomorphic quartz. Phenocrysts are found among this quartz. All the sandstones are poorly sorted except sandstone 1 which is moderately sorted. The mineralogical maturity of these sandstones is stable. Based on textural maturity, these sandstones are immature. According to the classification [5], they are ferruginous quartz wackes. These sandstones are derived from the gratification of clayey sand whose clay matrix has been oxidized [8]. Among these sandstones, two sandstones are porous (sandstone1 and sandstone) and the third one (sandstone3) is non-porous; the porous sandstones are made of three components (cement, pores, and grains), and the non-porous ones of two components (cement and grains). The pores of sandstones are intergranular and interconnected pores (Fig. 1); the cement is represented by black colour, the pores by blue, and the grains by white.
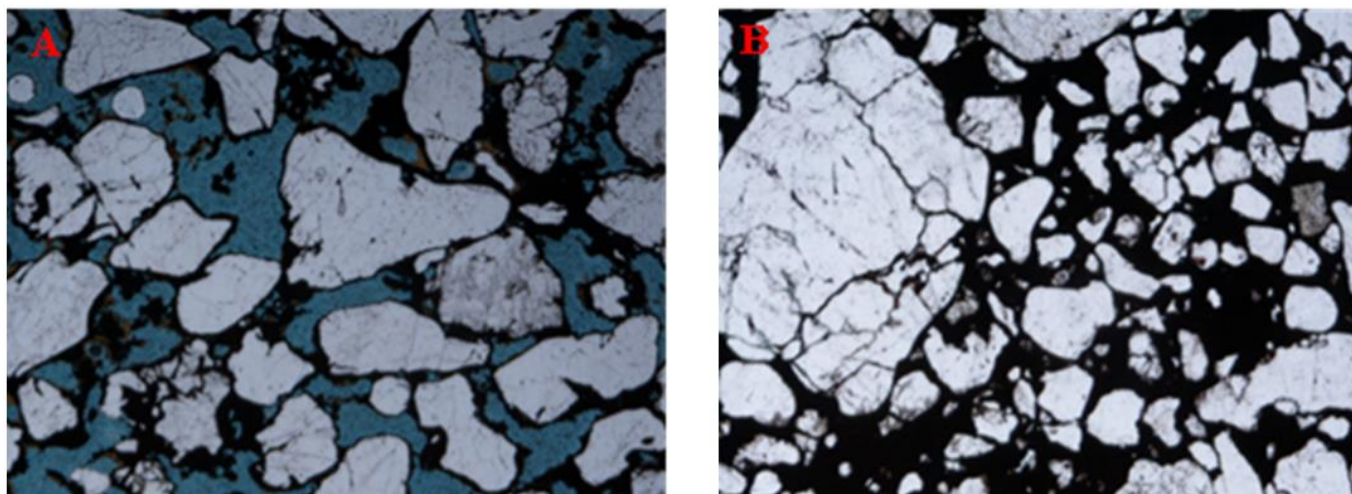
Fig. 1.   Ferruginous quartz wackes. A: Porous ferruginous quartz wackes and moderately sorted. B: Non-porous ferruginous quartz wackes and poorly sorted

3.1.2 SANDSTONE OF THE IVORIAN OFFSHORE BASIN

The sandstones in this part of the basin are mainly composed of monocrystalline quartz grains, rarely accompanied by oxidised glauconite grains. Quartz phenocrysts occur in some sandstones, and quartz grain outgrowth can be seen in some sandstones. The pores of these sandstones are mostly filled with a clay matrix which is oxidised in places to a ferruginous cement (Fig. 2). In this figure, the grains are in white, the pores in blue and the matrix and/or cement in black. The blue resin that occupies the pores is sometimes mixed with the matrix in some places in the sandstone. The pores are only present in sandstones4 and sandstone5; the matrix and/or cement are in small quantities. The sandstone6 is non-porous and consists of sometimes oxidised matrix and grains.

The sandstones of the offshore basin are well sorted (sandstone4) to poorly sorted (sandstone5 and sandstone6). Sandstone4 and sandstone5 are quartz arenite and sandstone7 is quartz wacke.
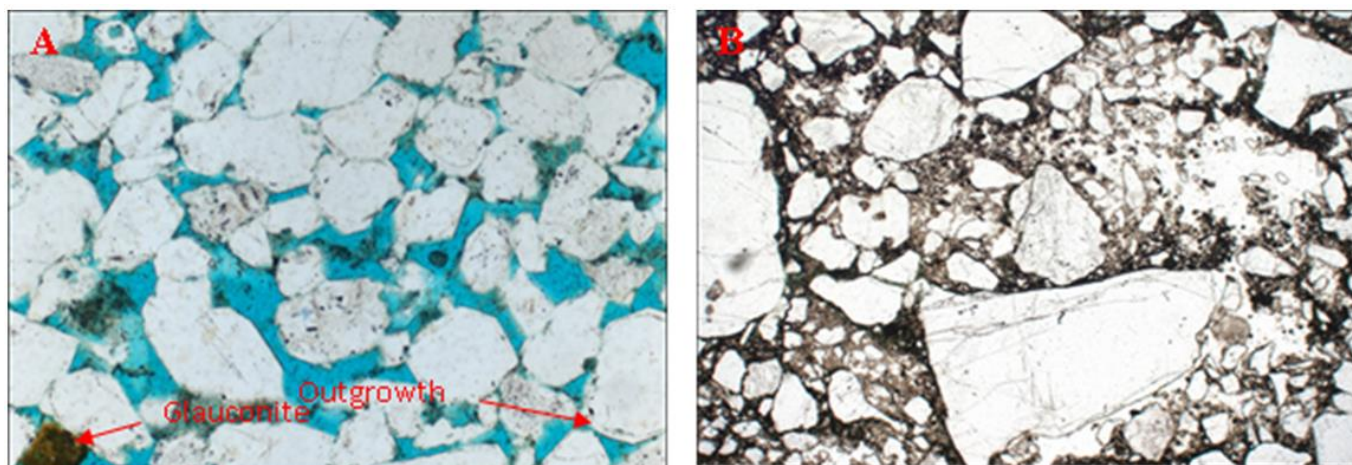
Fig. 2.   A: Well sorted and porous quartz arenite. B: Poorly sorted and non-porous quartz wacke.

3.2   TELE-PETROGRAPHY OF SANDSTONES

The image processing results in SpatRasters with four spectra (layers), three of which can be used to characterize the different components. The fusion of three layers gives a SpatRaster whose pixels are grouped in five intervals color. For each sandstone sample, two images were used for processing.

3.2.1   TELE-PETROGRAPHY OF SANDSTONES IN THE IVORIAN ONSHORE BASIN

TELE-PETROGRAPHY OF SANDSTONE 1

This sandstone is composed of three components, namely pores, cement and grains. The pores are interconnected and are represented in the images by blue colouring. Both images were taken at the same magnification.

The SpatRasters of two images of sandstone1 group the pixels (cells) into five colour intervals, of which one interval corresponds to the cement, two to the pores and two to the grains (Figures 3 and 5). The average sum of cells (pixels) in two images is 998199.5; the sandstone1_1 image has the higher sum (Tab. 1). The distribution of these cells in the cement, pores and grains of sandstone1 gives an average abundance of 47.29% grains, 30.77% pores and 21.95% cement (Tab. 1). The components are not uniformly distributed in the different areas of the sandstone1 based on the different values (Tab. 1).

The density curves of different images of sandstone1 show three modes reflecting the three components (cement, pores and grains). These density curves and their corresponding histograms also show that grains are the most dominant in the two sandstone1 images (Fig. 4 and 6). Although the cement mode is higher than the pore mode in the density diagram of sandstone1_1, the proportion of cement is still lower than that of pores; this is because the cement mode is leptokurtic (very sharp) and less dispersed (0 - 36.8) while the pore mode is more extensive (36.8 -110) with more cells.

Table 1.   Proportion of Components in the Sandstone 1

Statistics	Sandstone 1		Average
	sandstone1_1	sandstone1_2	
Sum	1001422	994977	998199.5
%Cement	25.13	18.77	21.95
%Pores	28.46	33.07	30.77
%Grains	46.41	48.16	47.29
%Total	100	100	100
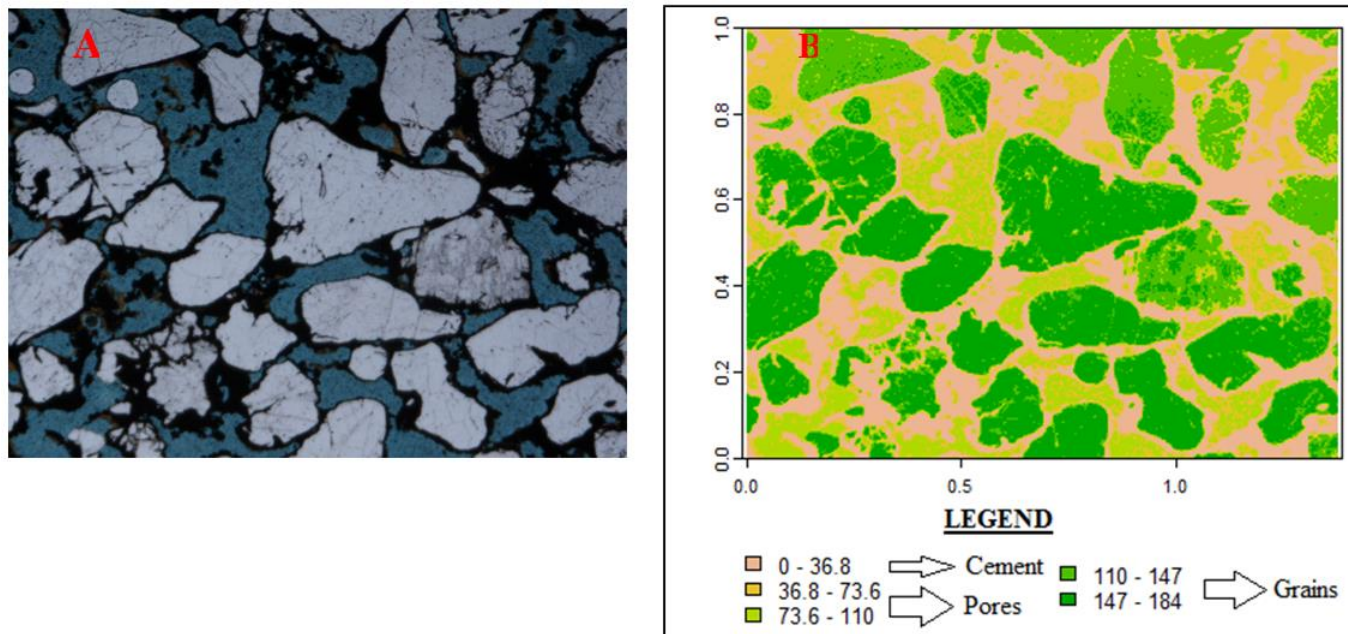
Fig. 3.   Image of Sandstone 1_1. A: Natural light. B: SpatRaster
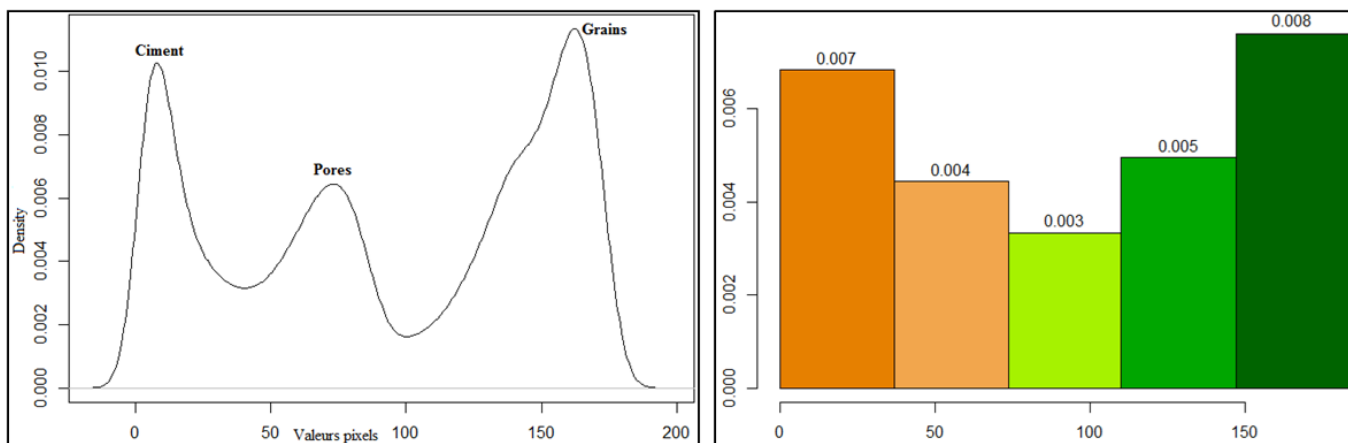
Fig. 4.   Density curve and histogram of Sandstone 1_1
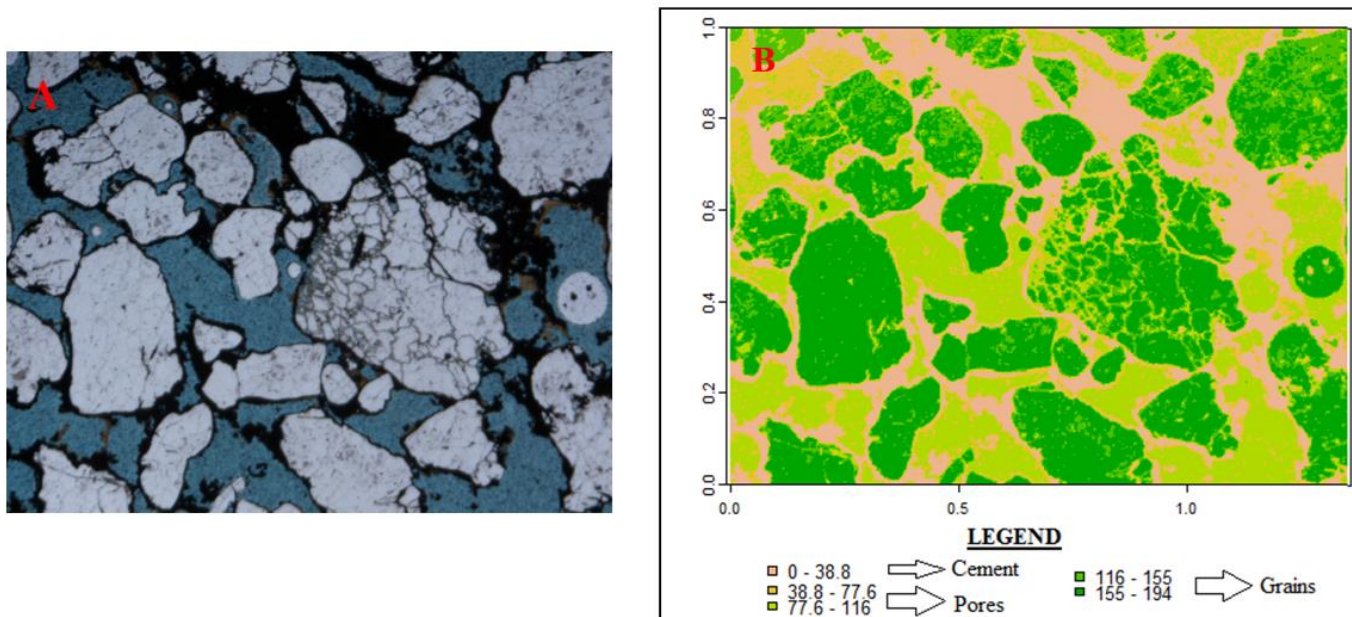
Fig. 5.   Image of Sandstone 1_2. A: Natural light. B: SpatRaster
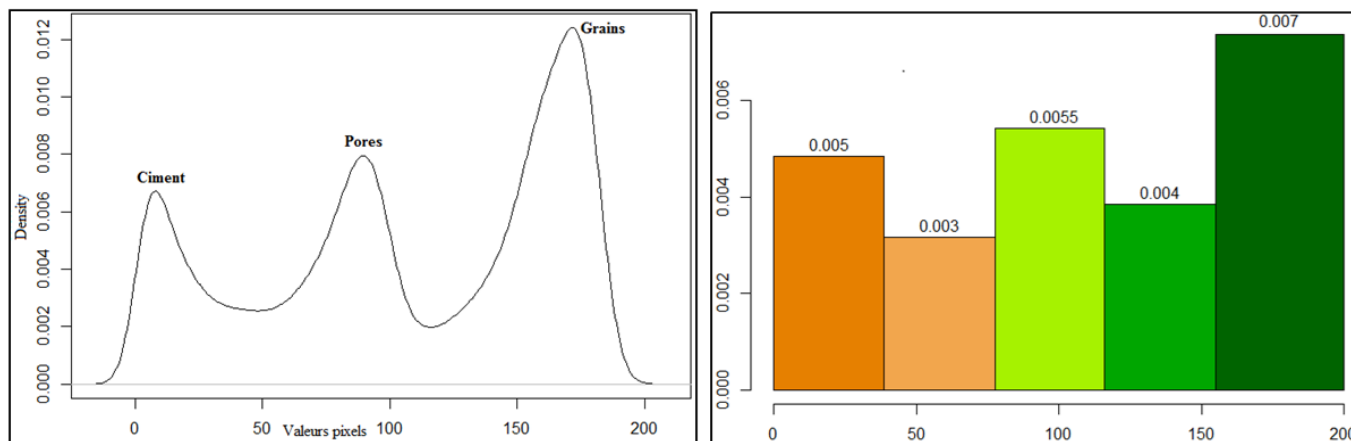
Fig. 6.   Density curve and histogram of sandstone 1_2

TELE-PETROGRAPHY OF SANDSTONE 2

The two images of sandstone 2 were also taken at the same magnification under transmitted light. The average cell sum (pixel) of the SpatRasters is 1001052. In the SpatRasters, the cement is located in one staining interval, the pores and grains in two intervals each (Fig. 7 and 9). Cement occupies on average 17.2% of the pixels, pores 45.28% and grains 37.53%. The pores are the most numerous on average (Tab. 2). But in image 2 of sandstone 2 (sandstone 2_2), grains dominate. This can be seen from the density curves and histograms, which also show the abundant proportions and the three components (Fig. 8 and 10).

Table 2.   Proportion of Components in the Sandstone 2

Statistics	Sandstone 2		Average
	Sandstone 2_1	Sandstone 2_2	
Sum	1000818	1001286	**1001052**
%Cement	14.04	20.35	**17.2**
%Pores	55.08	35.47	**45.28**
%Grains	30.88	44.18	**37.53**
%Total	100	100	**100**
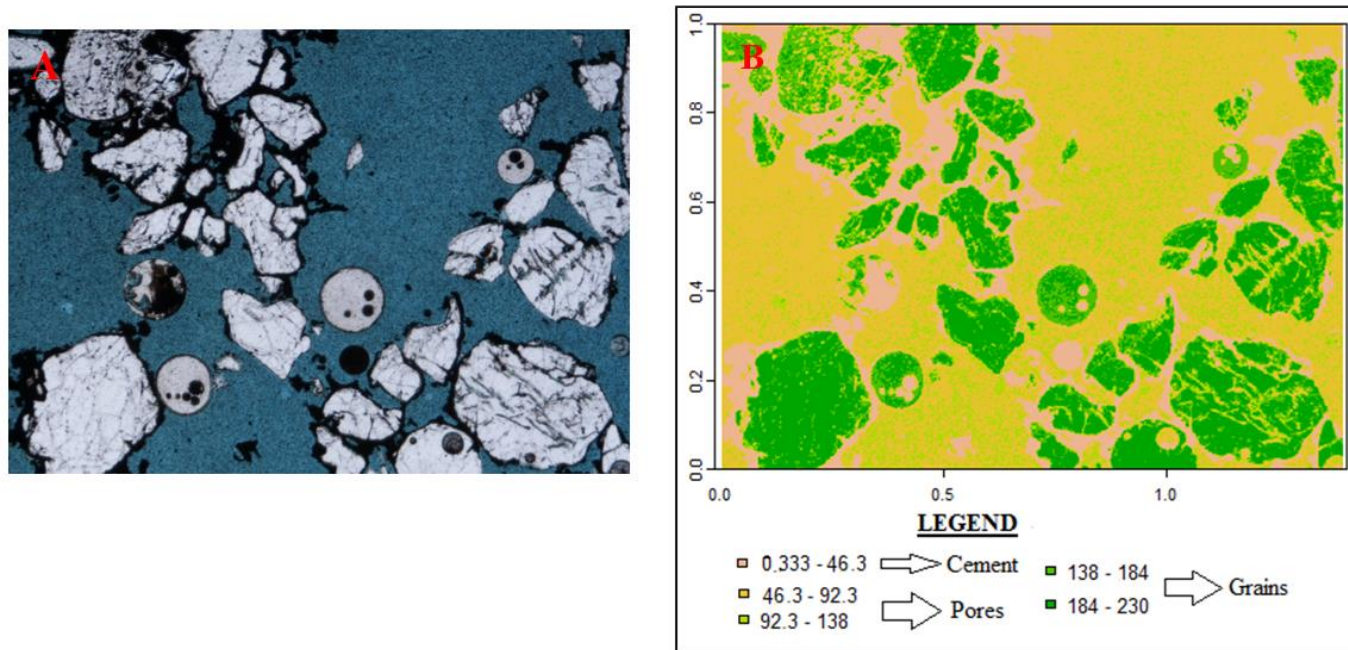
Fig. 7.   Image of Sandstone 2_1. A: Natural Light. B: SpatRaster
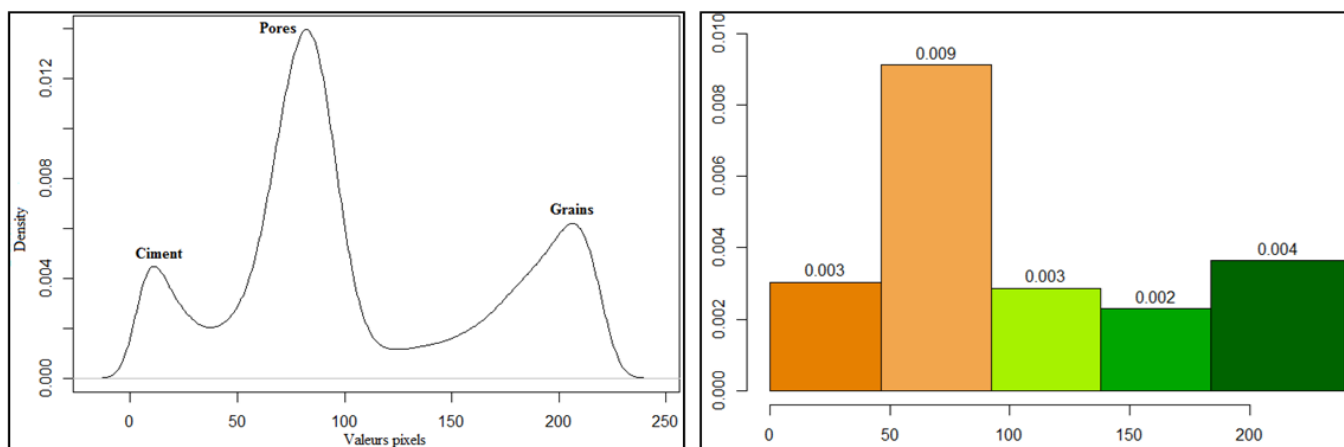
Fig. 8.   Density curve and histogram of sandstone 2_1
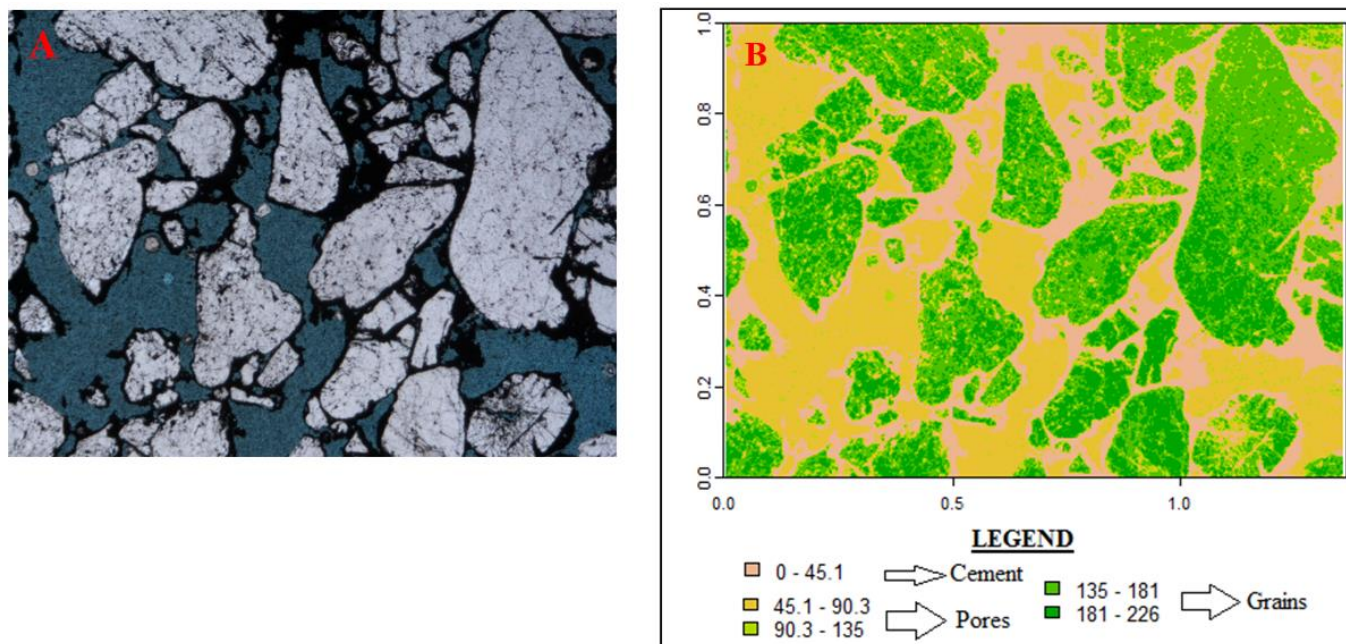
Fig. 9.   Image of Sandstone 2_2. A: Natural light. B: SpatRaster
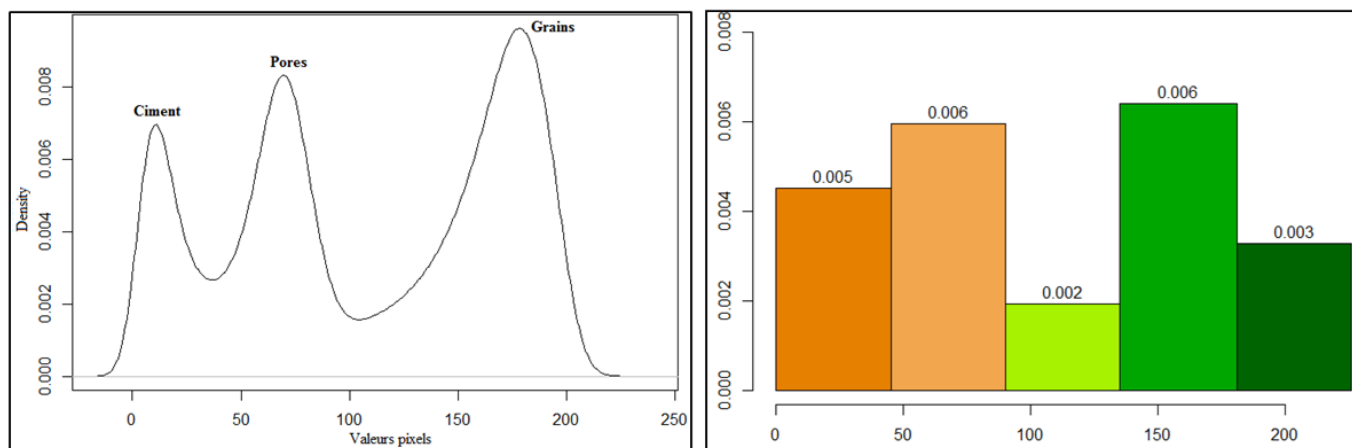
Fig. 10.   Density curve and histogram of sandstone 2_2

TELE-PETROGRAPHY OF SANDSTONE 3

The sandstone 3 is non-porous; it consists of cement and grains (quartz minerals). The SpatRasters pixels of the two images of this sandstone are grouped into five color intervals, of which two intervals correspond to cement and three to grains (Fig. 11 and 13). The average sum of the pixels is 1000770, of which the cement has an average of 42.78% and the grains 57.23% (Tab. 3).

Table 3.   Proportion of Components in the Sandstone 3

Statistics	Sandstone 3		Average
	Sandstone 3_1	Sandstone 3_2	
Somme	1000971	1000569	**1000770**
%Cement	40.18	45.37	**42.78**
%Grains	59.82	54.63	**57.23**
%Total	100	100	**100**

The density curves of the two sandstones also reveal two modes, one associated with cement and the other with grains. However, the cement mode is more important than the grain mode in both images. The cement pixel values are more concentrated between 0 and 50 while those of the grains are more spread out. This is further explained by the histograms which show the distribution of the pixels over the five intervals (Fig. 12 and 14).
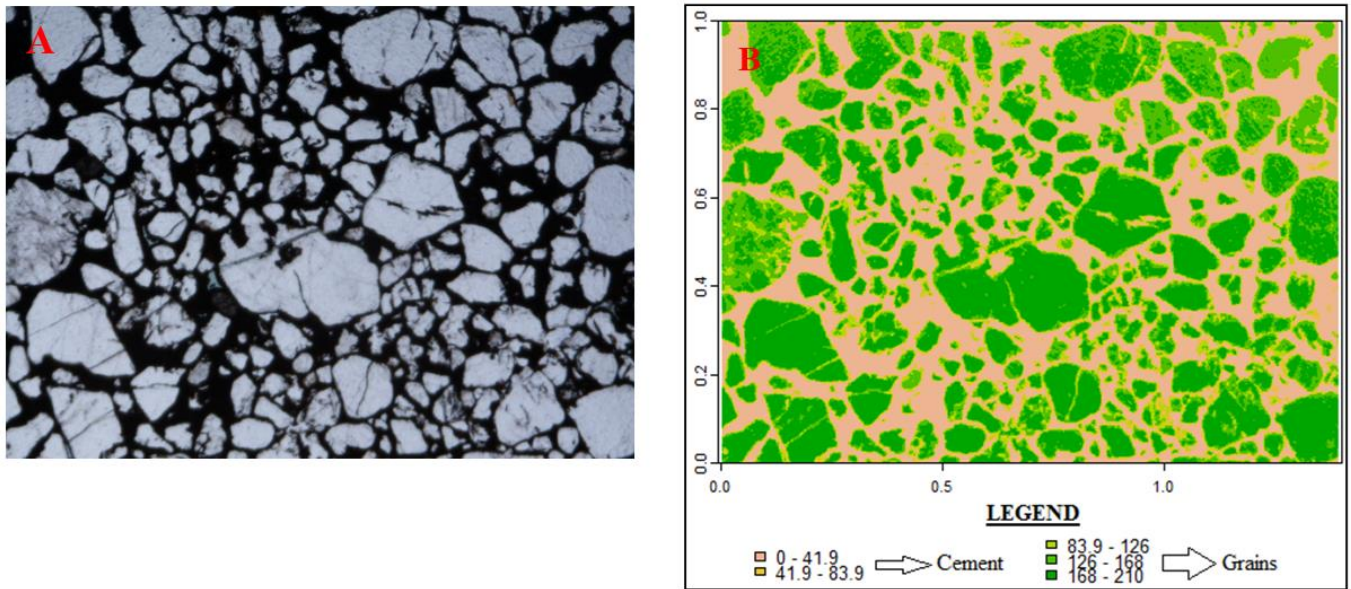
Fig. 11.   Image of Sandstone 3 _1. A: Natural light. B: SpatRaster
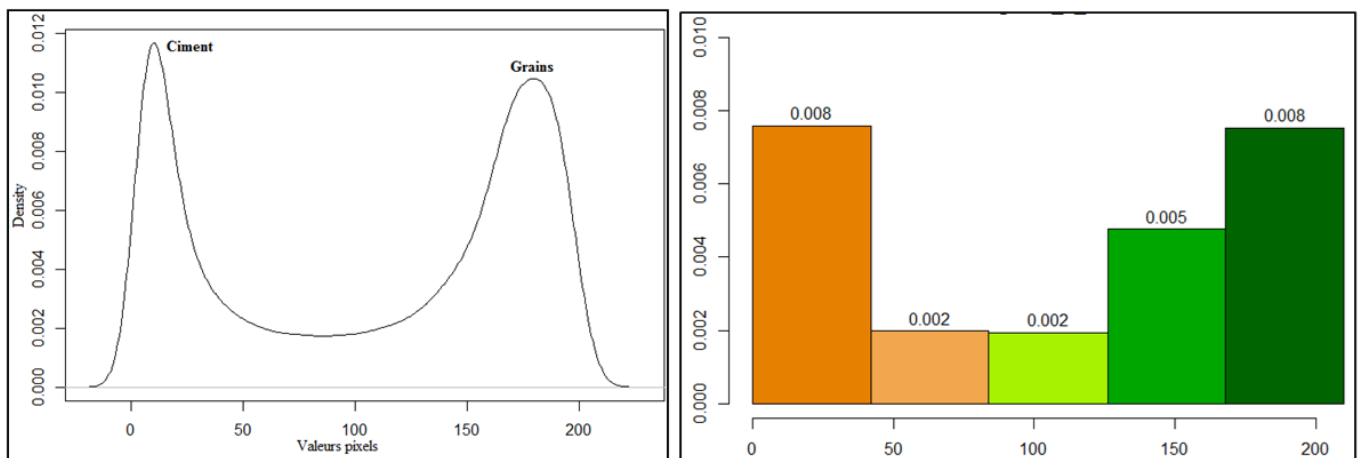
Fig. 12.   Density curve and histogram of Sandstone 3_1
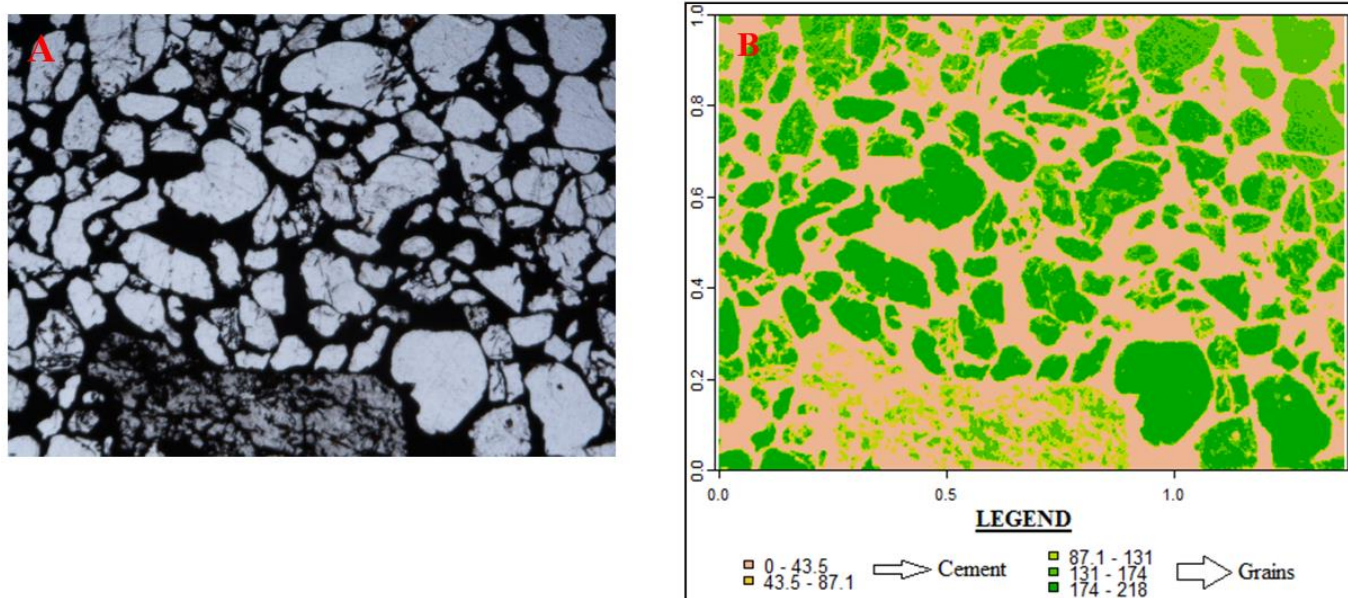
Fig. 13.   Image of Sandstones 3_2. A: Natural light. B: SpatRaster
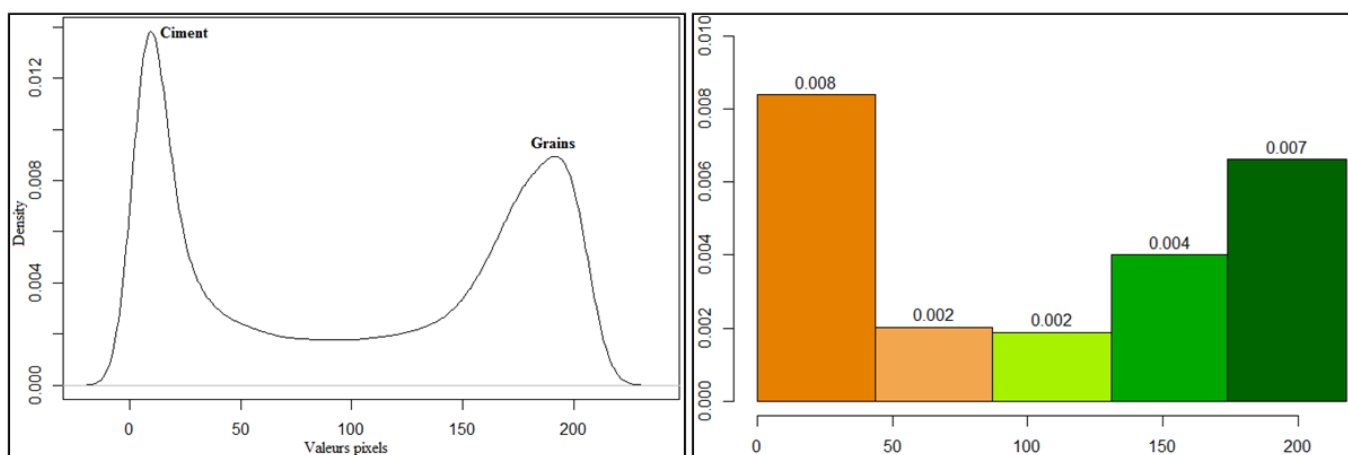
Fig. 14.   Density curve and histogram of Sandstone 3_2

3.2.2   TELE-PETROGRAPHY OF THE SANDSTONE OF THE IVORIAN OFFSHORE BASIN

TELE-PETROGRAPHY OF SANDSTONE 4

The two images of sandstone 4 were taken at different magnifications; sandstone 4_1 at medium magnification and sandstone 4_2 at high magnification. In the sandstone 4 images, four components can be distinguished, namely the cement (ferruginous and siliceous), the matrix (clay and oxidized glauconite), the pores and the grains (quartz minerals). The oxidation of the clay matrix gives the ferruginous cement and the outgrowth of the quartz gives the siliceous cement. In the natural light images of microscope, the ferruginous cement and the matrix are dark except for the oxidized glauconite which shows an orange coloration. The blue resin colors the pores and the quartz grains and siliceous cement are white. In the images, there is a localized fusion of the matrix and the blue-colored pores.

The pixels of the SpatRasters grouped in five color intervals reveal the dominance of quartz grains with an average proportion of 77.54% (two intervals). The pores have an average proportion of 12.74% (one interval). Ferruginous cement and matrix have an average proportion of 1.5% (one range) and 8.23% (one range) respectively (Tab. 4). The proportion of siliceous cement could not be evaluated due to a lack of differentiation from quartz grains as they have the same reflectance on SpatRasters. The average pixel sum is 514912.5.

On the SpatRaster of the sandstone 4_2 image, the grains, matrix and cement have higher proportions than on the sandstone 4_1 image. The opposite case occurs with the pores. The magnification of the microscope image has therefore an impact on the proportion of the elements and especially if there are phenocrysts (Fig. 15 and 17).

Table 4.   Proportion of Components in the Sandstone 4

Statistics	Sandstone 4		Average
	Sandstone 4_1	Sandstone 4_2	
Sum	428301	601524	514912.5
%Cement	1.08	1.92	1.5
%Matrix	5.52	10.94	8.23
%Pores	17.58	7.89	12.74
%Grains	75.82	79.25	77.54
%Total	100	100	100
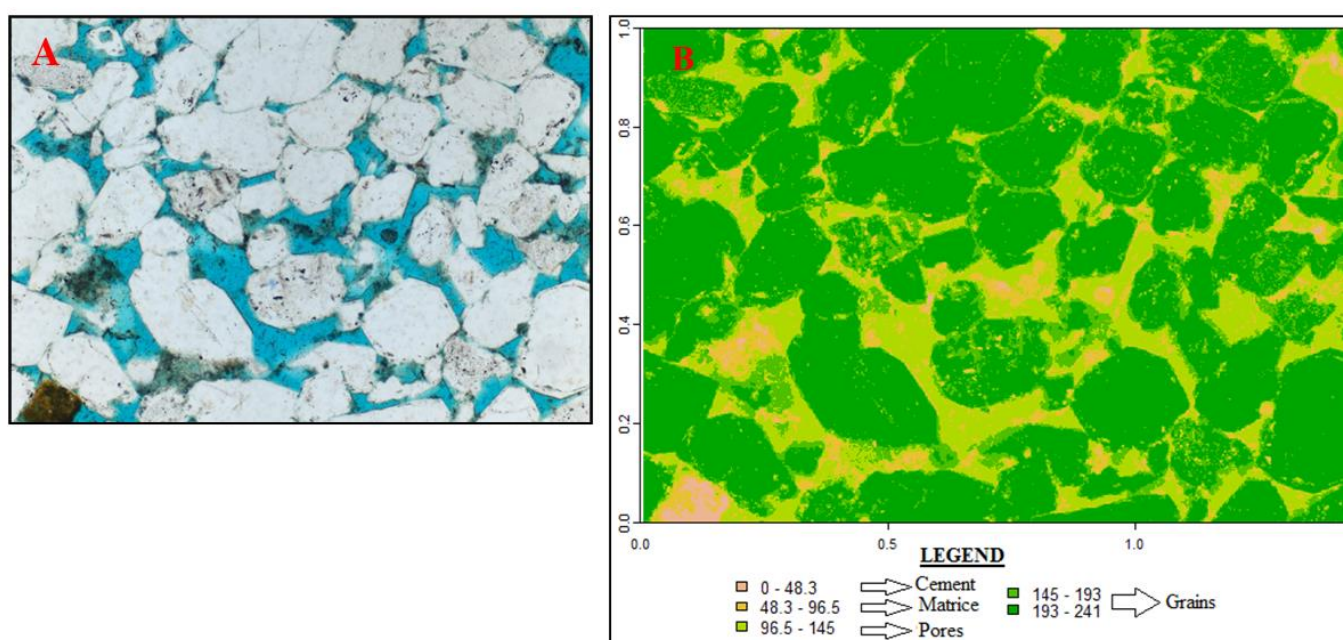
Fig. 15.   Image of Sandstone _1. A: Natural light. B: SpatRaster

The density curves and histograms show two modes in each of two images of sandstone 4. In the image of sandstone 4_1, the two modes only reveal the presence of pores and grains. In the second image, the matrix and the grains are highlighted. The low proportions of the components remain invisible on the density curves (Fig. 16 and 18).
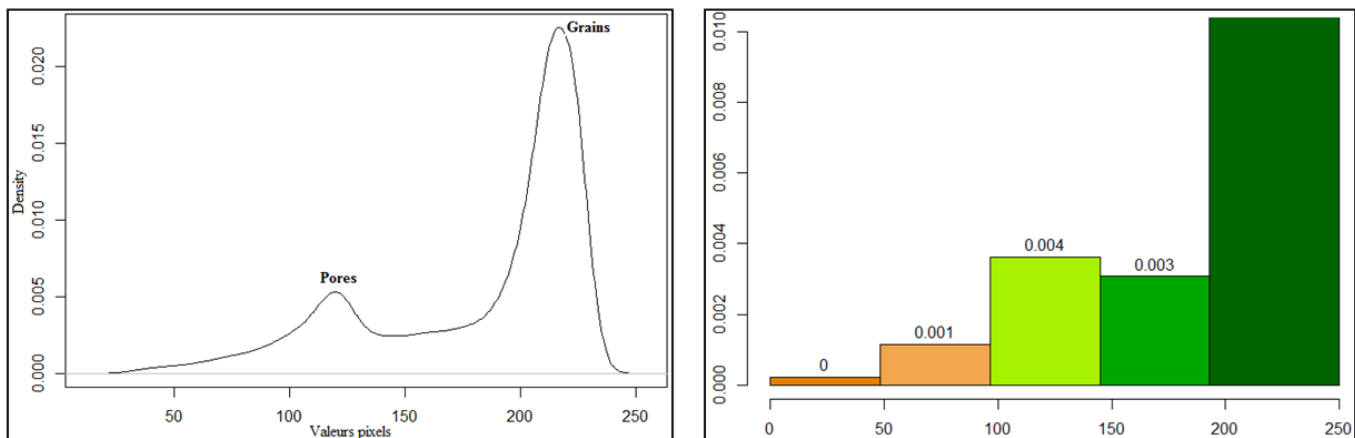
Fig. 16.   Density curve and histogram of Sandstone 4_1
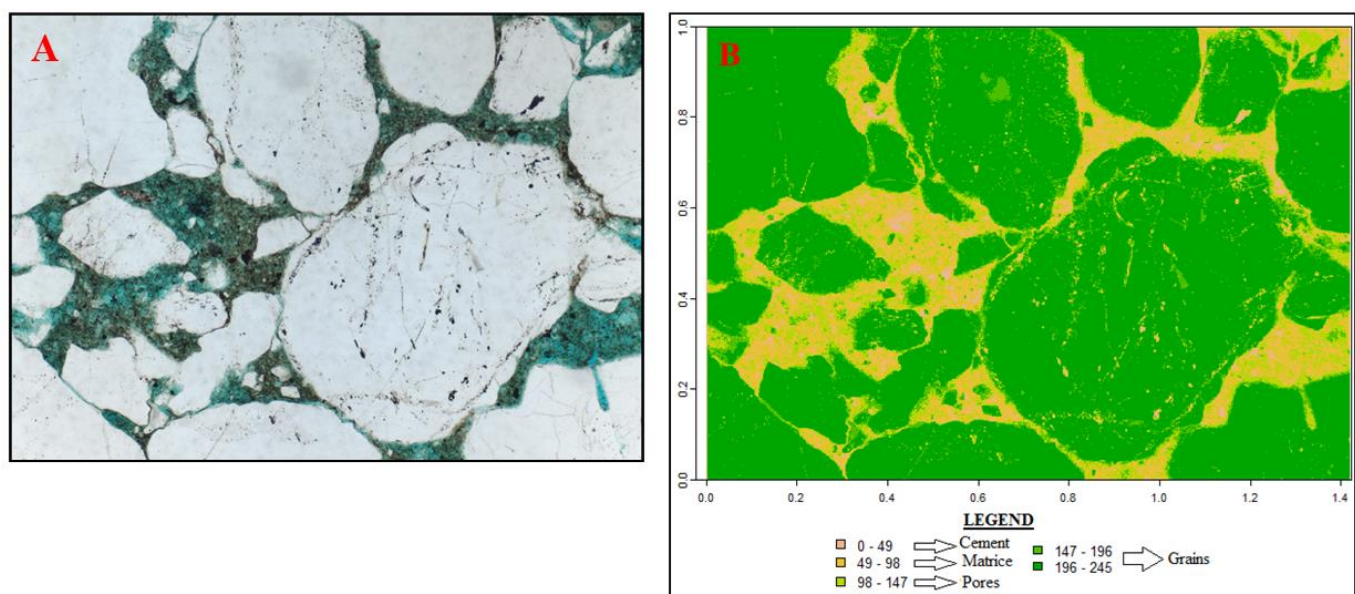
Fig. 17.   Image Sandstone 4 _2 with phenocrysts. A: Natural light. B: SpatRaster
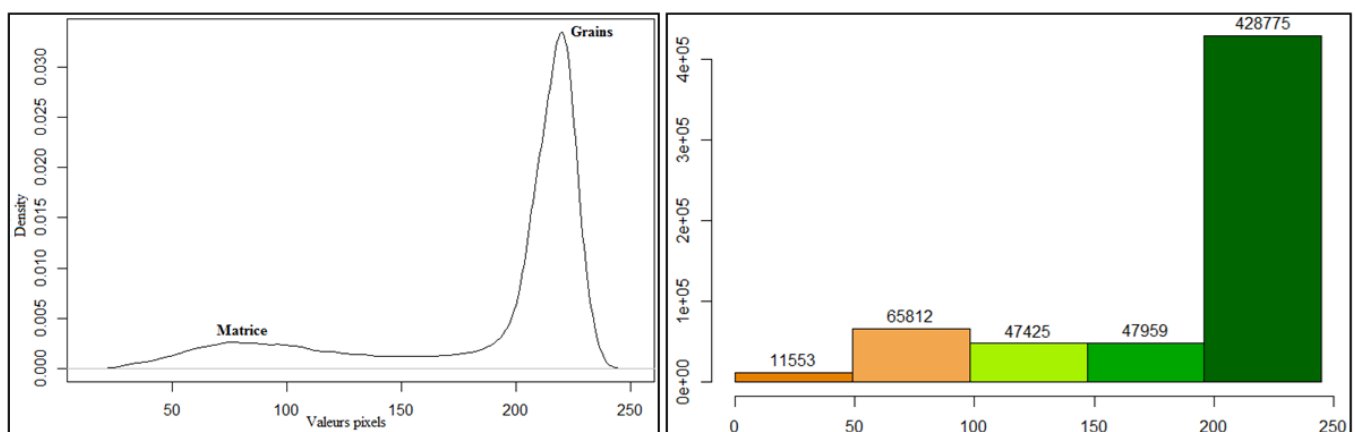
Fig. 18.   Density curve and histogram of Sandstone 4_2

TELE-PETROGRAPHY OF SANDSTONE 5

For this sandstone, one image was taken at low magnification and another at medium magnification. At low magnification, three components (cement, pores and grains) are identified while four components (cement, matrix, pores and grains) are revealed at high magnification. The cement and matrix have the same black coloration at low magnification, which produces the same reflectance on its SpatRaster image.

The SpatRaster of both images group the pixels (cells) into five color intervals. In the SpatRaster image of sandstone 5_1, one interval corresponds to cement, two to pores and two to grains (Fig. 19). On the other hand, in the SpatRaster image of sandstone 5_2, cement, matrix and pores belong to one-pixel value interval each, while grains belong to two intervals (Fig. 21). The SpatRaster was able to separate the matrix from the pores in the image of sandstone 5_2; the color representing the matrix is found under that of the pores in this image (Fig. 21B). The average cell (pixel) sum of the two images is 637804 (Tab. 5). The distribution of pixels in the cement, matrix, pores and grains gives an average of 4.29%, 4.64%, 28.34% and 62.74% respectively (Tab. 1). The matrix is not discriminated in the image of sandstone 5_1. The magnification of the microscope image also had an impact on the proportion of elements (Fig. 19 and 21).

Table 5.   Proportion of Components in the Sandstone 5

Statistics	Sandstone 5		Average
	Sandstone 5_1	Sandstone 5_2	
Sum	638168	637440	637804
%Cement	6.87	1.71	4.29
%Matrix	0	9.27	4.64
%Pores	34.93	21.74	28.34
%Grains	58.2	67.28	62.74
%Total	100	100	100

The density curves and histograms show two modes (pores and grains). The proportions of cement and matrix remain invisible on the density curves because their proportions are low (Fig. 20 and 22).
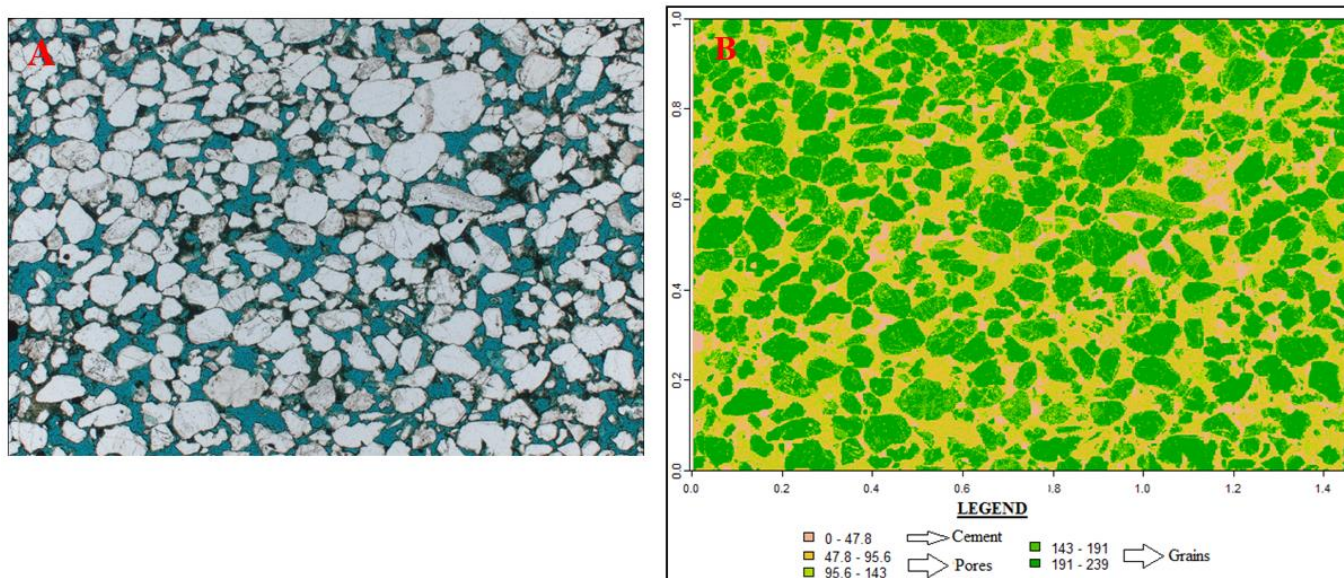
Fig. 19.   Image of Sandstone 5_1.: A: Natural light. B: SpatRaster
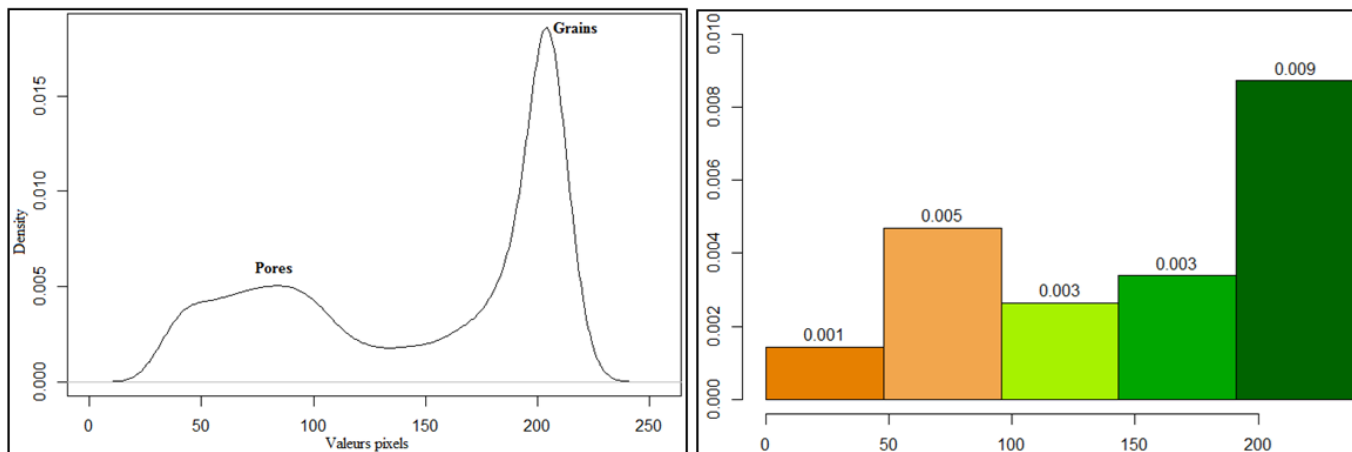
Fig. 20.   Density curve and histogram of Sandstone 5_1
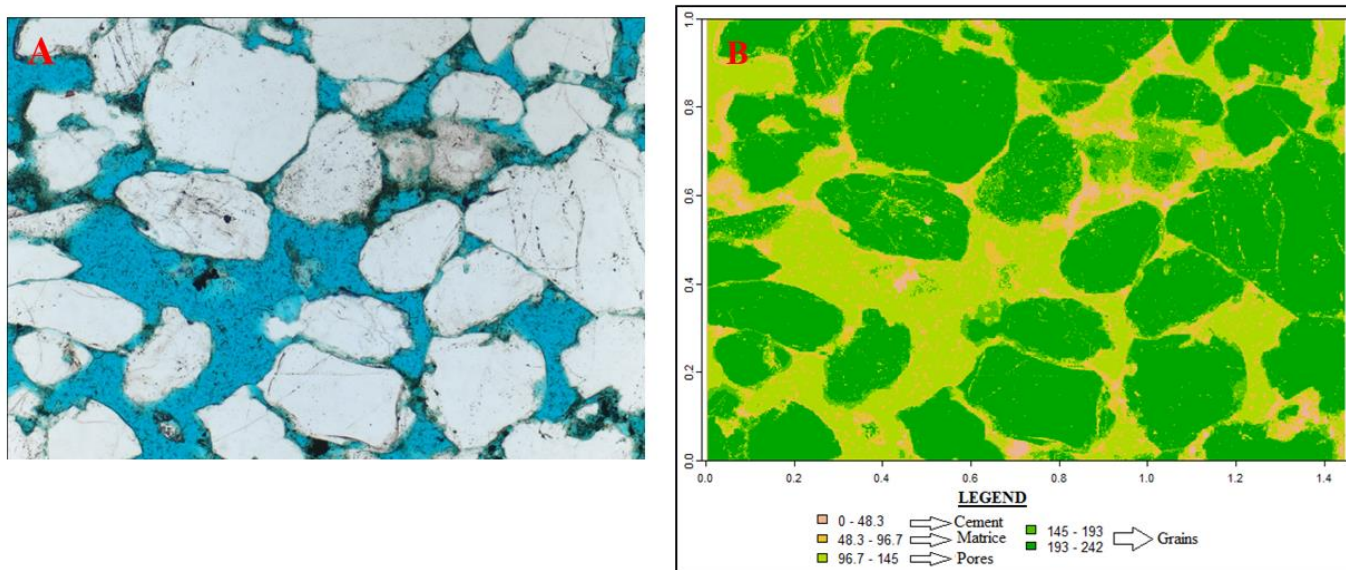
Fig. 21.   Image of Sandstone 5_2. A: Natural light. B: SpatRaster
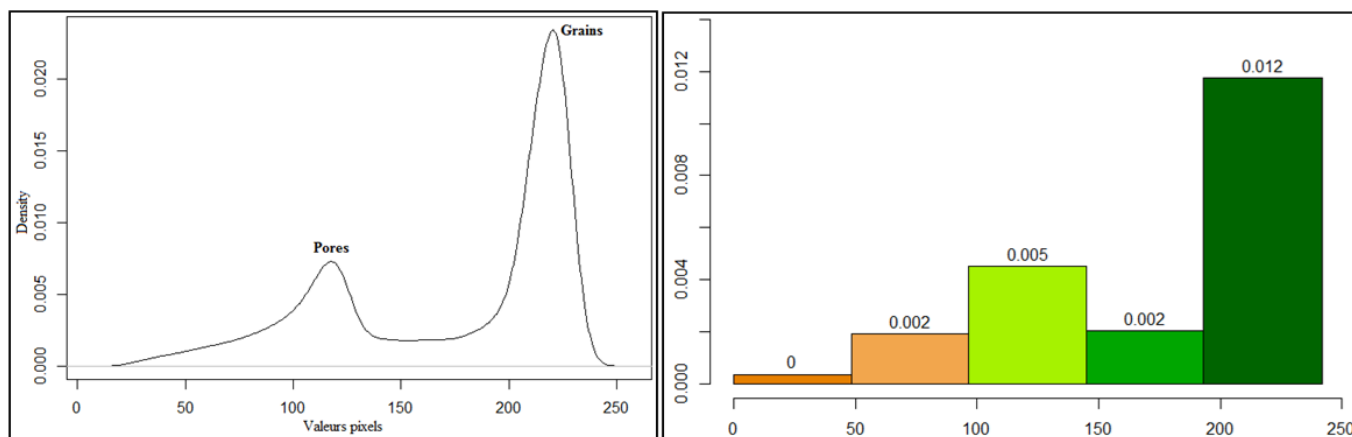
Fig. 22.   Density curve and histogram of Sandstone 5_2

TELE-PETROGRAPHY OF SANDSTONE 6

Sandstone 6 is non-porous and is characterized by three components: the cement, the clay matrix and the quartz grains. The two images of this sandstone were taken at the same magnification (high magnification) and it is the sandstone with the highest number of phenocrysts, hence the poorly sorting.

The SpatRasters of this sandstone group the layers into five color intervals of which one interval characterizes the cement, another the matrix and the remaining three the quartz grains (Fig. 23 and 25). The average pixel sum is 618330.5. The grains strongly dominate this sandstone with an average proportion of 81.28%. Cement and matrix have respectively average proportions of 7.46% and 11.27% (Tab. 6). We note that the more the phenocrysts are highlighted in the images, the more proportion of grains increases and conversely the proportion of cement and matrix decreases. The phenocrysts, therefore, influence the proportions of the components (Fig. 23 and 25).

The density curves and histograms reveal the presence of two modes, the smallest mode corresponding to the matrix and the largest to the grains. The proportion of cement remains invisible on the density curves because their proportions are low (Fig. 24 and 26).

Table 6.   Proportion of Components in the Sandstone 6

Statistics	Sandstone 6		Average
	Sandstone 6_1	Sandstone 6_2	
Sum	638028	598633	618330.5
%Cement	4.71	10.2	7.46
%Matrix	9.95	12.58	11.27
%Grains	85.34	77.22	81.28
%Total	100	100	100
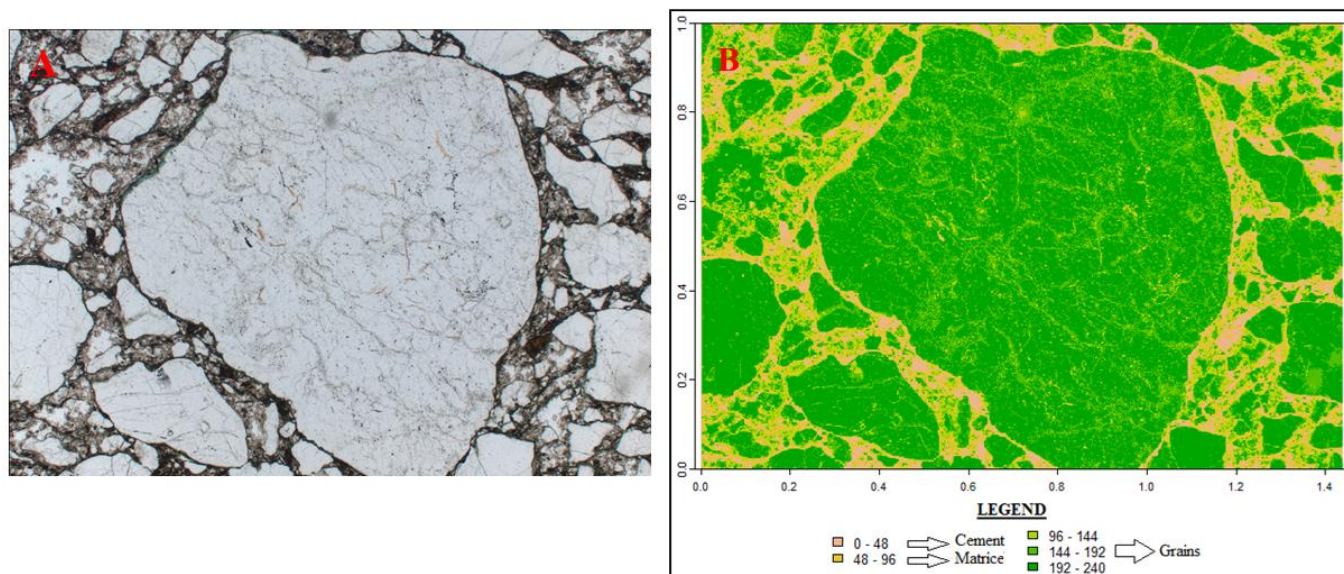
Fig. 23.   Image of Sandstone 6_1. A: Natural light. B: SpatRaster
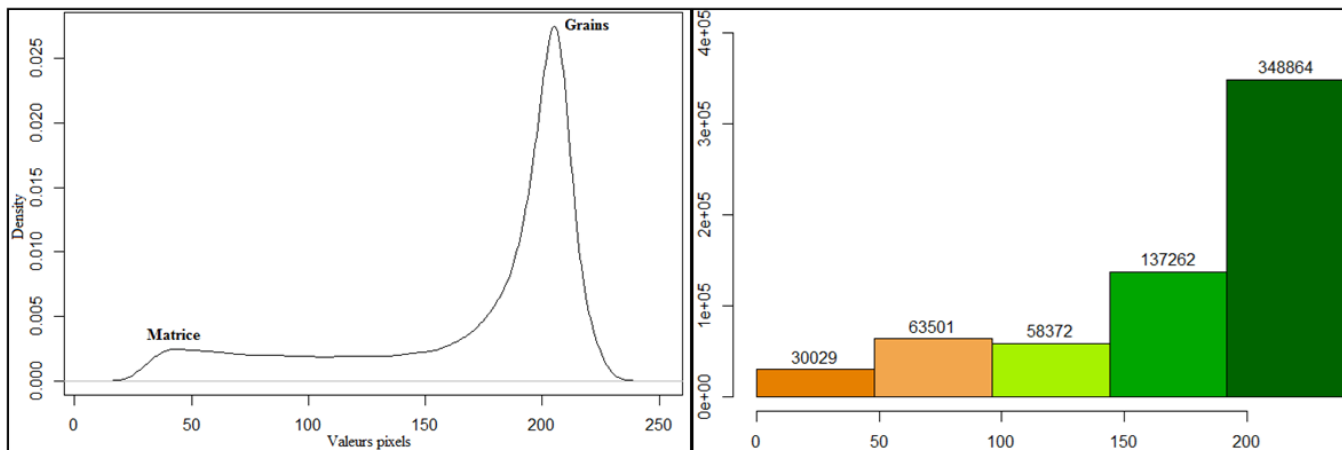
Fig. 24.   Density curve and histogram of Sandstone 6_1
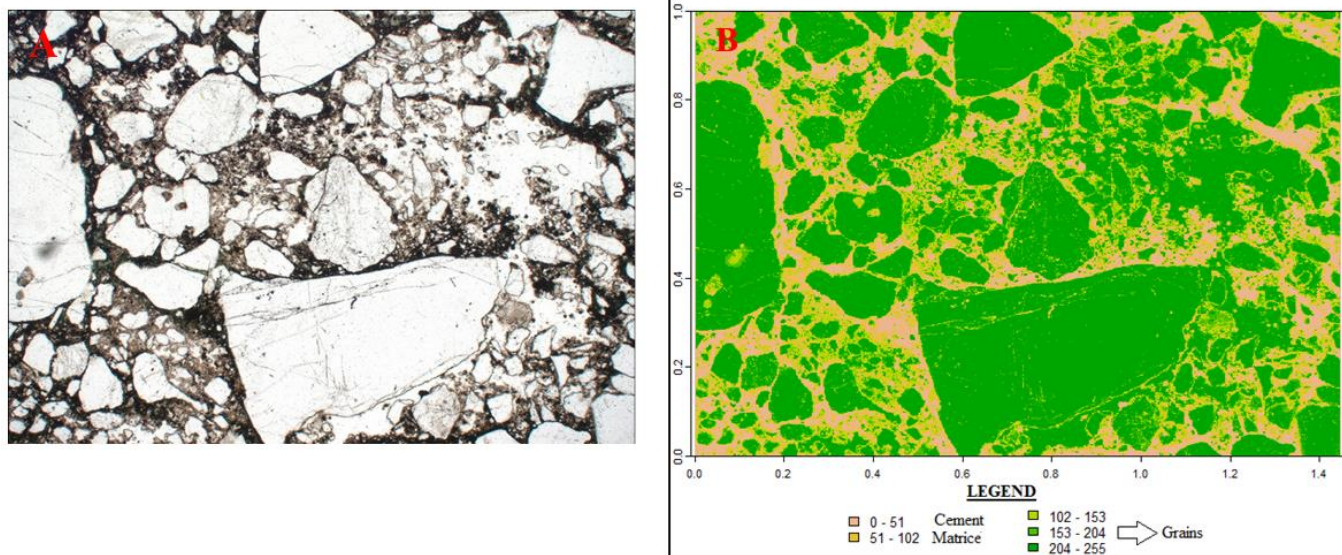
Fig. 25.   Image of Sandstone 6_2. A: Natural light. B: SpatRaster
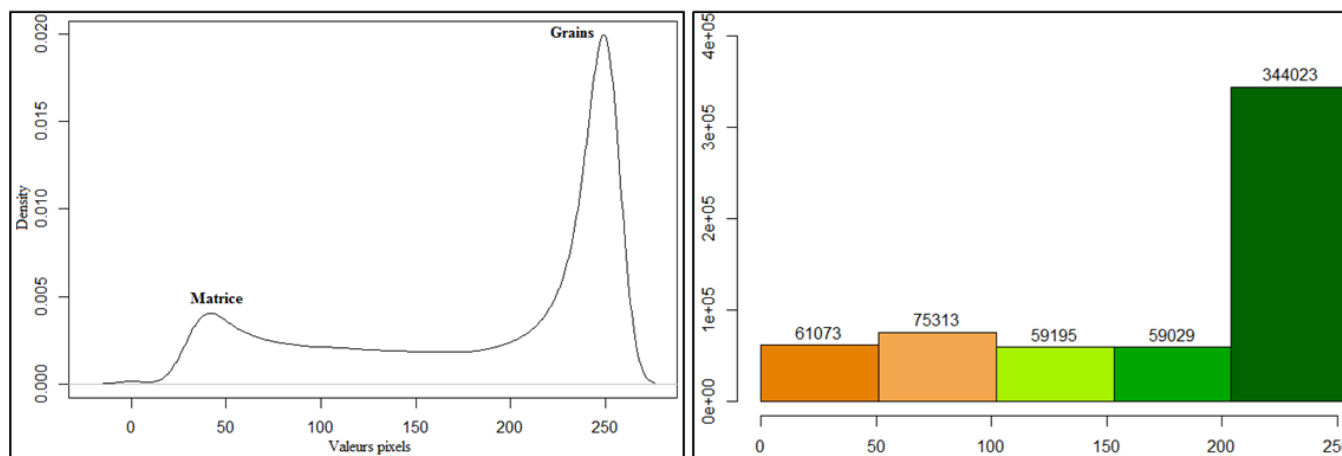
Fig. 26.   Density curve and histogram of Sandstone 6_2

4   DISCUSSION

The onshore quartz wackes comes from the ferruginisation of old superficial clayey sands. The kaolinitic clay matrix has been oxidised [8]. This transformation of clayey sands into quartz wackes occurred subsurface at the sediment-air interface; it is therefore an exogenetic cementation [9].

In the case of offshore sandstones, consolidation occurred by oxidation of the matrix but also by the outgrowth of quartz grains due to the pressure between the grains. This consolidation occurred long after the sediments were buried in the marine environment; the cementation is therefore described as mesogenetic cementation [9].

Porosity is greater in onshore sandstones (surficial rocks) than in the sandstone of offshore which are deeply buried. This difference is due to the degree of compaction which is more pronounced at depth than at the subsurface. In the images of the onshore sandstones, the grains barely touch each other (point contacts) whereas, in the offshore sandstones, the grains are more closely packed together. These sandstones show long contacts and concavo-convex contacts.

The evaluation of different sandstone components by tele-petrography depends on grain-size, sorting and magnification.

At the grain size level, if there is a uniform size distribution, the proportions of components will be the same at any point in the rock; this implies very well sorted grains according to the chart for visual estimation of sorting [2].

However, when the grains have different sizes and especially phenocrysts (poorly classified grains), the proportions of components vary from one surface of the rock to another. The presence of phenocrysts tends to overestimate the proportions of grains and underestimate the other proportions (porosity, cement and matrix). In this case, several images must be taken to obtain the average proportion. This phenomenon is more accentuated the higher the magnification of the microscope image. Low and medium magnifications give a larger observation area and therefore a reduced number of images per rock. Their only problems are in the discrimination of the different components. We have the example of sandstone5 where the matrix could not be separated from the cement because of the same coloring they showed at medium magnification. However, it could be separated from the cement at high magnification based on their different colorations.

Another problem in the tele-petrography study is the inability to differentiate between cement and minerals if they are of the same nature; this is the case with sandstones4 and sandstones5 where the quartz forms a growth to give a siliceous cement. In all cases, the proportion of pores will be known.

5   CONCLUSION

Tele-petrography is an indirect method capable of assessing the proportions of different components present in a rock. In the present work, this technique has allowed the quantitative evaluation of cement and/or matrix, pores and quartz grains in sandstones from the Ivorian basin.

The quantification of these components depends on the magnification of microscope image, the grain size and the sorting. Low and medium magnifications give larger areas of observation, resulting in fewer images per rock. These magnifications do not discriminate certain components such as cement and matrix. At higher magnifications, however, discrimination of these components is possible. In sandstones at well sorted, i.e. grains of approximately the same size, the proportions of components hardly vary from one image to another at any magnification. However, in poorly sorted sandstones (different sizes), the proportions vary from one image to another; this differentiation is more pronounced at higher magnification. The presence of phenocrysts also accentuates this differentiation, as they tend to overestimate the proportions of grains to the detriment of other components (porosity, cement and matrix).

The density curves and histograms highlight the number of components present in the rocks. However, the number on these curves depends of proportions; the higher the proportion of a component, the better it is represented on the curves. On the other hand, low proportions remain invisible on the density curves. For this sandstone study, only a maximum of three components were shown on the density curves, although in some sandstones there were four.

REFERENCES

[1] Hijmans. R. J., terra: Spatial Data Analysis, 2021b. [Online] Downloadable: https://CRAN.R-project.org/package=terra.

[2] Maurice E. T., Sedimentary Rocks in the Field. Third EDITION. Department of Geological Sciences University of Durham, UK. John Wiley& Sons Ltd, England, 234p, 2003.

[3] Gary N. S., Sedimentology and stratigraphy. Second edition. Wiley-Blackwell: A John Wiley& Sons, Ltd., Publication 111 River Street, Hoboken, USA, 419p, 2009.

[4] Adams A. E., Mackenzie W. S. &Guiford C., Atlas of sedimentary rocks under the microscope. Low-priced Edition. Longman Group UK Ltd, Longman House, Burnt Mill, Harlow, Essex CM 20 2JE, England, 104p, 1984.

[5] Pettijohn F. J., Potter P. E. &Siever R., Sand and Sandstone. In: Sedimentology and stratigraphy. Second edition. GARY N. S. Wiley-Blackwell: A John Wiley& Sons, Ltd., Publication 111 River Street, Hoboken, USA, pp. 5-86, 1987.

[6] Madelin, M., Analyse d'images raster et télédétection, 2021.
[Online] Downloadable: https://mmadelin.github.io/sigr2021/SIGR2021_raster_MM.html.

[7] Nowosad, J., Image processing and all things raster, 2021.
[Online] Downloadable: https://nowosad.github.io/SIGR2021/workshop2/workshop2.html.

[8] Assalé F. Y. P., Caractérisation sédimentologique, palynologique, géochimique et paléoenvironnementale des formations connexes à la faille des lagunes (Est du bassin onshore de Côte d'Ivoire). Thèse Doctorat uniq. Univ. F.H.B, Côte d'Ivoire, 361p, 2013.

[9] Scholle, P.A. & Ulmer-Scholle, D., Cements and cementation. In: Encyclopedia of Sediments and Sedimentary Rocks (Ed. Middleton, G.V.). Kluwer Academic Publishers, Dordrecht; pp. 110–119, 2003.